The Journal of Chemical Physics

# A pair natural orbital based implementation of CCSD excitation energies within the framework of linear response theory

Cite as: J. Chem. Phys. **148**, 134102 (2018); https://doi.org/10.1063/1.5018514
Submitted: 07 December 2017 . Accepted: 13 March 2018 . Published Online: 03 April 2018

Marius S. Frank, and Christof Hättig

View Online Export Citation CrossMark

ARTICLES YOU MAY BE INTERESTED IN

Linear response coupled cluster theory with the polarizable continuum model within the singles approximation for the solvent response
The Journal of Chemical Physics **148**, 134113 (2018); https://doi.org/10.1063/1.5021781

QED effects on individual atomic orbital energies
The Journal of Chemical Physics **148**, 134101 (2018); https://doi.org/10.1063/1.5026193

Communication: An improved linear scaling perturbative triples correction for the domain based local pair-natural orbital based singles and doubles coupled cluster method [DLPNO-CCSD(T)]
The Journal of Chemical Physics **148**, 011101 (2018); https://doi.org/10.1063/1.5011798

PHYSICS TODAY WHITEPAPERS
ADVANCED LIGHT CURE ADHESIVES
Take a closer look at what these environmentally friendly adhesive systems can do
READ NOW
PRESENTED BY MASTERBOND

AIP Publishing



© 2018 Author(s).

# A pair natural orbital based implementation of CCSD excitation energies within the framework of linear response theory

Marius S. Frank[a] and Christof Hättig[b]
*Lehrstuhl für Theoretische Chemie, Ruhr-Universität Bochum, D-44801 Bochum, Germany*

(Received 7 December 2017; accepted 13 March 2018; published online 3 April 2018)

We present a pair natural orbital (PNO)-based implementation of coupled cluster singles and doubles (CCSD) excitation energies that builds upon the previously proposed state-specific PNO approach to the excited state eigenvalue problem. We construct the excited state PNOs for each state separately in a truncated orbital specific virtual basis and use a local density-fitting approximation to achieve an at most quadratic scaling of the computational costs for the PNO construction. The earlier reported excited state PNO construction is generalized such that a smooth convergence of the results for charge transfer states is ensured for general coupled cluster methods. We investigate the accuracy of our implementation by applying it to a large and diverse test set comprising 153 singlet excitations in organic molecules. Already moderate PNO thresholds yield mean absolute errors below 0.01 eV. The performance of the implementation is investigated through the calculations on alkene chains and reveals an at most cubic cost-scaling for the CCSD iterations with the system size. *Published by AIP Publishing.* https://doi.org/10.1063/1.5018514

## I. INTRODUCTION

One of the severe limitations for computational chemistry is the steep scaling of the required computational resources (i.e., time and memory demands) of accurate wavefunction-based methods with the system size $\mathcal{N}$. This unphysical behavior arises from the fact that the canonical molecular orbitals (MOs) are delocalized. The non-local MO basis makes it difficult to exploit that dynamic electron correlation is a local phenomenon and decays with the interelectronic distance $R$ as $R^{-6}$.

Local correlation methods exploit the sparsity of electron correlation by neglecting excitations between spatially distant MOs. This is achieved by a transformation of the occupied orbitals to a localized MO (LMO) basis and by restricting excitations to a subspace of the full virtual space, i.e., to local correlation domains. Different local correlation methods mainly differ by the way the virtual subspaces are determined and represented. Pioneering work on these methods has been done by Saebø and Pulay[1–6] by introducing projected atomic orbitals (PAOs) as representation for the virtual space. Later, Werner, Schütz, and co-workers[7–12] implemented, refined, and extended these ideas to linear-scaling local coupled cluster (CC) methods implemented in the Molpro[13] package. An alternative approach to exploit the locality of electron correlation uses pair natural orbitals (PNOs) where each pair of occupied orbitals gets its own virtual space assigned which is truncated based on an analysis of approximate densities. The idea was already proposed and implemented in the 1970s by Meyer,[14–17] Ahlrichs,[18,19] Kutzelnigg,[18] and Staemmler and co-workers[18,20] but was then discontinued due to large computational demands for the transformation of two-electron integrals from the atomic orbital (AO) to the PNO basis. In 2008, Neese *et al.* realized that the aforementioned computational bottleneck can be circumvented by making use of the resolution-of-the-identity (RI) approximation[21,22] also known as density-fitting (DF). Combining the PNO and PAO approaches led Neese and co-workers to the development of improved linear scaling coupled cluster variants.[23–28]

Werner and co-workers[29] as well as Hättig and co-workers[30,31] proposed to use orbital specific virtuals[32] (OSVs) as an intermediate basis to reduce the computational costs for the construction of PNOs. An advantage of OSVs is that they share many properties with PNOs and can straightforwardly be generalized to different orbital spaces which is exploited in explicitly correlated F12 variants of PNO-MPn and PNO-CC methods.[30,33–35] This is also crucial for PNO-based coupled cluster response methods with state- or perturbation-specific PNOs and OSVs.[36–38]

The extension of PAO-based local correlation methods to excited states in the framework of response theory is not straightforward since excitation processes are usually delocalized over at least one chromophore. Describing ground and excited states with common domains for the virtual space would result in huge correlation domains that would need to contain local and non-local excitations (depending on the character of the excited states) and would grow in size with the number of states included. Apart from the CC2 method,[39,40] where an explicit treatment of the double excitation space can be avoided by partitioning techniques, the development of PAO-based response methods, e.g., coupled cluster singles and doubles (CCSD),[41,42] has been given up.

[a]Author to whom correspondence should be addressed: Marius.Frank@rub.de
[b]christof.haettig@rub.de

Dutta *et al.* recently presented an implementation[43] of equation of motion CCSD (EOM-CCSD) for excitation energies where domain-based local PNO-CCSD (DLPNO-CCSD) is used to solve the ground state amplitude equations with linear-scaling costs in the PNO basis and then the cluster amplitudes and other intermediates are back-transformed to the canonical virtual basis, the so-called back-transformed PNOs (bt-PNOs). The excited state problem is then solved in the canonical basis. This approach requires only minor modifications of an existing canonical code. On the other hand, it only reduces the prefactor of the computational costs but not the scaling with the system size. Combining the bt-PNO approach with similarity transformed EOM-CCSD (STEOM-CCSD) reduces the cost scaling but sacrifices important advantages of EOM-CCSD as, e.g., a qualitatively correct description of double excitations and its black-box character due to the introduction of an active space for single excitations.

Multilevel coupled cluster methods[44] also aim at a reduction of the prefactor of the computational costs. They divide the orbital space into active and inactive MOs which are treated at different levels of coupled cluster theory. Myhre and Koch[45] presented a multilevel CC3 model where CCSD is used for the inactive orbital space while the (smaller) active orbital space is treated at the computationally more demanding CC3 level. Even though this leads to a significant reduction of the prefactor of the computational costs, it does not reduce the steep scaling of the costs with the size of the chromophore and partially sacrifices the black-box character of the standard coupled-cluster methods.

Approaches to reduce the computational costs of coupled cluster response methods for excitation energy calculations that employ natural orbitals[46] and natural transition orbitals (NTOs)[47] either do not achieve the cost reductions and the compactness of the wavefunction parameters of PNO-based methods or only yield computational savings for local excitations which limits their applicability.

Hättig and Helmich,[36] in contrast, proposed to solve the eigenvalue problem for the excitation energies in a state-specific PNO basis to fully exploit the compactness of the parameter space that is achieved with PNOs in coupled cluster response calculations. In this approach, the excited state PNOs are generated separately for each excited state from densities calculated from configuration interaction singles with perturbative doubles [CIS(D)]-like doubles amplitudes. The number of amplitudes then scales linearly with the chromophore size and, equally important, the PNO truncation errors are small and decrease rapidly[36] for the perturbative CIS(D) method as well as for the iterative second order methods ADC(2) and CC2.[37] At the example of ADC(2)-x, it was furthermore shown that this strategy can straightforwardly be applied to higher-order methods with a non-diagonal doubles-doubles block of the Jacobian matrix. The most important feature of the state-specific PNO ansatz is that there are no conceptual limitations to achieve linear scaling operation counts and memory and disk space demands. In the present paper, we report the extension of this approach to the CCSD model including an analysis of the convergence of the PNO truncation errors with the occupation number threshold and demonstrate its computational efficiency compared to a canonical implementation.

## II. THEORY AND IMPLEMENTATION

### A. The coupled cluster singles and doubles model

In the following, we follow the notation introduced by Christiansen *et al.*[48] for the coupled cluster singles and doubles (CCSD) model[49–53] within the framework of linear response theory. In the CCSD model, the cluster operator is truncated after the double excitation operator $T_2$. This leads to the following cluster equations for the singles and doubles amplitudes:[54]

$$\Omega_{\mu_1} = \langle \mu_1 | \hat{H} + [\hat{H}, T_2] | \mathrm{HF} \rangle, \tag{1}$$

$$\Omega_{\mu_2} = \langle \mu_2 | \hat{H} + [\hat{H}, T_2] + \frac{1}{2}[[\hat{H}, T_2], T_2] | \mathrm{HF} \rangle, \tag{2}$$

where the $T_1$-similarity transformed Hamiltonian[54]

$$\hat{H} = e^{-T_1} H e^{T_1} = \sum_{pq} \hat{h}_{pq} E_{pq} + \sum_{pqrs} (pq\hat{|}rs) e_{pqrs}, \tag{3}$$

with $T_1 = \sum_{\mu_1} t_{\mu_1} \tau_{\mu_1}$ and $T_2 = \sum_{\mu_2} t_{\mu_2} \tau_{\mu_2}$, has been used. Here and in the following we present the equations for the closed-shell case and use the spin-free one- and two-electron operators $E_{pq}$ and $e_{pqrs}$ and the excitation operators $\tau_{ai} = E_{ai}$ and $\tau^{ij}_{ab} = E_{ai}E_{bj}$. Greek letters denote atomic orbitals (AOs), Latin letters denote molecular orbitals (MOs), and capital letters $P$, $Q$ auxiliary functions. The indices $\mu_1$ and $\mu_2$ run over, respectively, all single and double replacements.

The $T_1$-transformed integrals $\hat{h}_{pq}$ and $(pq\hat{|}rs)$ can be evaluated from the respective AO integrals using $\mathbf{t}_1$-dressed particle and hole MO transformation matrices,[54]

$$\mathbf{\Lambda}^p = \mathbf{C}\left(\mathbf{1} - \mathbf{t}_1^T\right), \tag{4}$$

$$\mathbf{\Lambda}^h = \mathbf{C}\left(\mathbf{1} + \mathbf{t}_1\right), \tag{5}$$

as

$$(pq\hat{|}rs) = \sum_{\mu\nu\kappa\lambda} \Lambda^p_{\mu p} \Lambda^p_{\nu r} \Lambda^h_{\kappa q} \Lambda^h_{\lambda s} (\mu\kappa|\nu\lambda). \tag{6}$$

The matrix $\mathbf{t}_1$ in the above equations is defined as[54]

$$\mathbf{t}_1 = \begin{pmatrix} 0 & 0 \\ \{t^i_a\} & 0 \end{pmatrix}. \tag{7}$$

In response theory, excitation energies are obtained as eigenvalues of the Jacobian,[55] which for CCSD is readily obtained from the cluster equations (1) and (2) as[48]

$$A_{\mu_i \nu_j} = \frac{\partial \Omega_{\mu_i}}{\partial t_{\nu_j}} = \begin{pmatrix} \langle \mu_1 | [\hat{H} + [\hat{H}, T_2], \tau_{\nu_1}] | \mathrm{HF} \rangle & \langle \mu_1 | [\hat{H}, \tau_{\nu_2}] | \mathrm{HF} \rangle \\ \langle \mu_2 | [\hat{H} + [\hat{H}, T_2], \tau_{\nu_1}] | \mathrm{HF} \rangle & \langle \mu_2 | [\hat{H} + [\hat{H}, T_2], \tau_{\nu_2}] | \mathrm{HF} \rangle \end{pmatrix}. \tag{8}$$

The eigenvalue problem is solved iteratively—usually using a block Davidson algorithm[56]—which requires an implementation of linear transformations of trial vectors with the Jacobian,

$$\rho_{\mu_i} = \sum_{\nu_j} A_{\mu_i\nu_j} R_{\nu_j}. \tag{9}$$

To obtain a compact notation for the transformed vectors $\rho_{\mu_i}$, we introduce the operators $R_i = \sum_{\mu_i} R_{\mu_i}\tau_{\mu_i}$ and the $R_1$-dressed Hamiltonian

$$\bar{H} = \left[\hat{H}, R_1\right] = \sum_{pq} \bar{h}_{pq} E_{pq} + \sum_{pqrs} (pq|\bar{r}s) e_{pqrs}, \tag{10}$$

with corresponding integrals

$$(pq|\bar{r}s) = P^{pr}_{qs} \sum_{\mu\nu\kappa\lambda} \left(\bar{\Lambda}^p_{\mu p}\Lambda^h_{\nu q} + \Lambda^p_{\mu p}\bar{\Lambda}^h_{\nu q}\right) \Lambda^p_{\kappa r}\Lambda^h_{\lambda s}(\mu\nu|\kappa\lambda), \tag{11}$$

and modified particle/hole MO transformation matrices

$$\bar{\Lambda}^p_{\mu a} = -\sum_i R^i_a C_{\mu i}, \tag{12}$$

$$\bar{\Lambda}^h_{\mu i} = \sum_a R^i_a C_{\mu a}. \tag{13}$$

In Eq. (11), the symmetrization operator $P^{qs}_{pr}$ is defined by $P^{qs}_{pr} f^{qs}_{pr} = f^{pr}_{qs} + f^{sq}_{rp}$. With this notation the transformed vectors $\rho_{\mu_i}$ can be written as

$$\rho_{\mu_1} = \langle\mu_1|\bar{H} + [\bar{H}, T_2] + [\hat{H}, R_2]|\mathrm{HF}\rangle, \tag{14}$$

$$\rho_{\mu_2} = \langle\mu_2|\bar{H} + [\bar{H}, T_2] + [\hat{H} + [\hat{H}, T_2], R_2]|\mathrm{HF}\rangle. \tag{15}$$

### B. Ground and excited state PNOs

PNOs are defined as linear combinations of virtual orbitals

$$|\bar{a}_{ij}\rangle = \sum_a |a\rangle d^{ij}_{a\bar{a}}, \tag{16}$$

where the expansion coefficients are the elements of the eigenvectors of the contribution $D^{ij}_{ab}$ of a LMO pair $ij$ to a one-electron density matrix,

$$\sum_{ab} d^{ij}_{a\bar{a}} D^{ij}_{ab} d^{ij}_{b\bar{b}} = n^{ij}_{\bar{a}} \delta_{\bar{a}\bar{b}}. \tag{17}$$

Here and in the following, indices $i$, $j$, $k$, $l$ denote occupied orbitals, $a$, $b$, $c$, $d$ virtuals and PNOs and OSVs are denoted by, respectively, bar and tilde accents.

For the ground state, $D^{ij}_{ab}$ are approximate MP2 densities calculated as

$$D^{ij}_{ab} = 2\sum_c \left(\tilde{t}^{ij,(1)}_{ac} t^{ij,(1)}_{bc} + \tilde{t}^{ij,(1)}_{ca} t^{ij,(1)}_{cb}\right), \tag{18}$$

with $\tilde{t}^{ij,(1)}_{ab} = 2t^{ij,(1)}_{ab} - t^{ij,(1)}_{ba}$ and the first order amplitudes

$$t^{ij,(1)}_{ab} = \frac{(ai|bj)}{F_{ii} + F_{jj} - \epsilon_a - \epsilon_b}, \tag{19}$$

where $F_{ii}$ are the diagonal Fock matrix elements in a localized molecular orbital (LMO) basis and $\epsilon_a$ are canonical orbital energies.

For excited state PNOs, the MP1 ground state amplitudes in Eq. (18) are replaced by first-order doubles amplitudes

$$R^{ij,(1)}_{ab} = \frac{(ai|\bar{b}j)}{F_{ii} + F_{jj} - \epsilon_a - \epsilon_b + \omega} \tag{20}$$

calculated in a CIS(D)-like way from the current guess for the excitation energy $\omega$ and the singles amplitudes via the $R_1$-transformed integrals $(ai|\bar{b}j)$. The pair density is then constructed analogously to the ground state as

$$D^{ij}_{ab} = 2\sum_c \left(\tilde{R}^{ij,(1)}_{ac} R^{ij,(1)}_{bc} + \tilde{R}^{ij,(1)}_{ca} R^{ij,(1)}_{cb}\right), \tag{21}$$

with $\tilde{R}^{ij,(1)}_{ab} = 2R^{ij,(1)}_{ab} - R^{ij,(1)}_{ba}$. In addition, pairs for which the second-order correlation energy contribution evaluated with $t^{ij,(1)}_{ab}$ for the ground state and with $R^{ij,(1)}_{ab}$ for excited states is less than a pair energy threshold $T_{pair}$ are discarded.

The construction of the pair densities has the complexity $\mathcal{O}(\mathcal{N}^5)$ if done for all pairs $ij$ and in the full virtual basis. To reduce the complexity the pair densities are constructed in a preselected pair-specific semi-canonical pre-PNO basis $\{\tilde{a}_{ij}\}$ obtained by merging the OSV spaces for the LMOs $i$ and $j$ and then diagonalizing the Fock matrix in this space. The approximate doubles amplitudes for Eqs. (18) and (21) are then evaluated as

$$t^{ij,(1)}_{\tilde{a}_{ij}\tilde{b}_{ij}} = \frac{(\tilde{a}_{ij}i|\tilde{b}_{ij}j)}{F_{ii} + F_{jj} - \epsilon_{\tilde{a}_{ij}} - \epsilon_{\tilde{b}_{ij}}}, \tag{22}$$

$$R^{ij,(1)}_{\tilde{a}_{ij}\tilde{b}_{ij}} = \frac{(\tilde{a}_{ij}i|\bar{\tilde{b}}_{ij}j)}{F_{ii} + F_{jj} - \epsilon_{\tilde{a}_{ij}} - \epsilon_{\tilde{b}_{ij}} + \omega}, \tag{23}$$

where $\epsilon_{\tilde{a}_{ij}}$ are the eigenvalues of the Fock matrix in the pre-PNO basis.

In addition we pre-screen the list of pairs $ij$ based on an estimate for the second-order pair contributions to the correlation energies for the ground $e^{(2)}_{ij}$ or the excited state $\omega^{(2)}_{ij}$ which is evaluated in the OSV basis,

$$e^{(2)}_{ij} = \sum_{\tilde{a}_i\tilde{b}_j} \frac{(\tilde{a}_i i|\tilde{b}_j j)^2}{F_{ii} + F_{jj} - \epsilon_{\tilde{a}_i} - \epsilon_{\tilde{b}_j}}, \tag{24}$$

$$\omega^{(2)}_{ij} = \sum_{\tilde{a}_i\tilde{b}_j} \frac{(\tilde{a}_i i|\bar{\tilde{b}}_j j)^2}{F_{ii} + F_{jj} - \epsilon_{\tilde{a}_i} - \epsilon_{\tilde{b}_j} + \omega}. \tag{25}$$

The ground state pairs with $e^{(2)}_{ij} < \frac{1}{3}T_{pair}$ and the excited state pairs with $\omega^{(2)}_{ij} < \frac{1}{3}T_{pair}$ are discarded. The factor $\frac{1}{3}$ ensures that in this step no pairs are discarded for which the more accurate pair correlation energy estimates obtained from $t^{ij,(1)}_{ab}$ for the ground state and from $R^{ij,(1)}_{ab}$ for excited states are above $T_{pair}$.

Combined with a local RI approximation this leads to a quadratic cost scaling of the PNO construction for ground and excited states.[31,37,57]

TABLE I. Explicit expressions for the contributions to the doubles result vector. $\rho_{\mu_2}$ is split into contributions as $\rho_{\mu_2} = \rho^A_{\mu_2} + \rho^B_{\mu_2} + \rho^C_{\mu_2} + \rho^D_{\mu_2} + \rho^E_{\mu_2} + \rho^F_{\mu_2}$ and $P_{ij}$ is a permutation operator defined by $P_{ij} f_{ij} = f_{ji}$.

| Contribution | Scaling CCSD | Scaling PNO-CCSD |
|---|---|---|
| $\rho^{A,ij}_{\bar{a}\bar{b}} = \sum_{kl} \Gamma^{T_2+E,ij}_{kl} \sum_{\bar{a}'} S^{ij,kl}_{\bar{a}\bar{a}'} \sum_{\bar{b}'} S^{ij,kl}_{\bar{b}\bar{b}'} R^{kl}_{\bar{a}'\bar{b}'}$ $+ \sum_{kl} \Gamma^{R_2+\bar{E},ij}_{kl} \sum_{\bar{a}^0} S^{ij,kl}_{\bar{a}\bar{a}^0} \sum_{\bar{b}^0} S^{ij,kl}_{\bar{b}\bar{b}^0} t^{kl}_{\bar{a}^0\bar{b}^0}$ $+ \sum_{kl} t^k_{\bar{a}} t^l_{\bar{b}} \sum_{\bar{c}\bar{d}} R^{ij}_{\bar{c}\bar{d}} \sum_{\bar{c}^0\bar{d}^0} S^{ij,kl}_{\bar{c}\bar{c}^0} K^{kl}_{\bar{c}^0\bar{d}^0} S^{kl,ij}_{\bar{d}^0\bar{d}}$ | $\mathcal{O}(\mathcal{N}^6)$ | $\mathcal{O}(\mathcal{N})$ |
| $\rho^{B,ij}_{\bar{a}\bar{b}} = \sum_{\bar{c}\bar{d}} R^{ij}_{\bar{c}\bar{d}} (\bar{a}\bar{c}\vert\bar{b}\bar{d}) - P^{ij}_{\bar{a}\bar{b}} \sum_k t^k_{\bar{b}} \Omega^{B(R2),ij}_{\bar{a}k} - P^{ij}_{\bar{a}\bar{b}} \sum_k R^k_{\bar{a}} \Omega^{B(T2),ij}_{k\bar{b}}$ | $\mathcal{O}(\mathcal{N}^4)$ | $\mathcal{O}(\mathcal{N}^2)$ |
| $\rho^{C,ij}_{\bar{a}\bar{b}} = -P^{ij}_{\bar{a}\bar{b}} \left(\frac{1}{2} + P_{ij}\right) \sum_k \sum_{\bar{c}} C^{ik}_{\bar{a}_{ij}\bar{c}_{kj}} \sum_{\bar{b}'} R^{jk}_{\bar{c}\bar{b}'} S^{jk,ij}_{\bar{b}'\bar{b}}$ $- P^{ij}_{\bar{a}\bar{b}} \left(\frac{1}{2} + P_{ij}\right) \sum_k \sum_{\bar{c}^0} \bar{C}^{ik}_{\bar{a}_{ij}\bar{c}^0_{kj}} \sum_{\bar{b}^0} t^{jk}_{\bar{c}^0\bar{b}^0} S^{jk,ij}_{\bar{b}^0\bar{b}}$ | $\mathcal{O}(\mathcal{N}^6)$ | $\mathcal{O}(\mathcal{N})$ |
| $\rho^{D,ij}_{\bar{a}\bar{b}} = \frac{1}{2} P^{ij}_{\bar{a}\bar{b}} \sum_k \sum_{\bar{c}} D^{ik}_{\bar{a}_{ij}\bar{c}_{kj}} \sum_{\bar{b}'} \tilde{R}^{jk}_{\bar{c}\bar{b}'} S^{jk,ij}_{\bar{b}'\bar{b}}$ $+ \frac{1}{2} P^{ij}_{\bar{a}\bar{b}} \sum_k \sum_{\bar{c}^0} \bar{D}^{ik}_{\bar{a}_{ij}\bar{c}^0_{kj}} \sum_{\bar{b}^0} \tilde{t}^{jk}_{\bar{c}^0\bar{b}^0} S^{jk,ij}_{\bar{b}^0\bar{b}}$ | $\mathcal{O}(\mathcal{N}^6)$ | $\mathcal{O}(\mathcal{N})$ |
| $\rho^{E,ij}_{\bar{a}\bar{b}} = P^{ij}_{\bar{a}\bar{b}} \sum_{\bar{c}} R^{ij}_{\bar{a}\bar{c}} \sum_b d^{ij}_{b\bar{b}} \sum_c E_{bc} d^{ij}_{c\bar{c}}$ $+ P^{ij}_{\bar{a}\bar{b}} \sum_{\bar{a}^0} S^{ij,ij}_{\bar{a}\bar{a}^0} \sum_{\bar{c}^0} t^{ij}_{\bar{a}^0\bar{c}^0} \sum_b d^{ij}_{b\bar{b}} \sum_c \bar{E}_{bc} d^{ij}_{c\bar{c}^0}$ | $\mathcal{O}(\mathcal{N}^5)$ | $\mathcal{O}(\mathcal{N}^3)$ |
| $\rho^{F,ij}_{\bar{a}\bar{b}} = (\bar{a}i\vert\bar{b}j)$ | $\mathcal{O}(\mathcal{N}^4)$ | $\mathcal{O}(\mathcal{N})$ |

### C. Implementation of transformations with the CCSD Jacobian in a PNO basis

For the transformations with the CCSD Jacobian, we follow a similar approach as proposed by Christiansen *et al.*,[48] i.e., we introduce global ($t_{\mu_i}$-dependent) intermediates, which are only computed once after the ground state CC equations are converged, and local ($R_{\mu_i}$-dependent) intermediates, which have to be computed for each trial vector. For an easier discussion, we split the doubles part of the transformed vector $\rho_{\mu_2}$ into contributions denoted by $\rho^A_{\mu_2}$, $\rho^B_{\mu_2}$, ..., $\rho^F_{\mu_2}$ (compare Table I).

To account for the different pair lists in ground and excited states and the state-specific PNOs, some of the $t_{\mu_i}$-dependent intermediates become state specific and are recomputed for each state and whenever the excited state PNO basis is updated (*vide infra*). To distinguish between the different PNO basis sets we denote in the following ground state PNOs with $\bar{a}^0$ and excited state PNOs with $\bar{a}$.

The implementation of the CCSD ground state equations has been described in the context of PNO-CCSD[F12] in Ref. 34. The CCSD singles part of the transformed vectors is evaluated in the same way as for CC2. Therefore, we do not repeat the equations here but refer to Ref. 37 for further details. Table I summarizes how the contributions to the double excitation part of the transformed vectors $\rho_{\mu_2}$ are evaluated with state-specific PNOs. The intermediates used in Table I are defined in Tables III and IV in the Appendix. We follow a similar route as proposed by Neese and co-workers[23] for the residual of the ground state amplitude equations: The general strategy of the implementation is to pre-compute all integrals and intermediates for the Jacobian transformations which do not depend on $R_{\mu_i}$ prior to the Davidson procedure. Depending on the intermediates this is done for the ground or the excited state PNO basis and/or the respective pair lists. Some intermediates, as, e.g., the overlap matrices $S^{ij,kl}_{\bar{c}\bar{c}^0}$ and the intermediates $\bar{C}^{ik}$ and $\bar{D}^{ik}$ for the ring terms, are needed with some indices in the ground and some indices in the excited state PNO basis and for a combination of the respective pair lists. During the evaluation of the result vector $\rho_{\mu_2}$, the amplitudes and intermediates are in some places projected from the PNO space of a pair $ij$ to the PNO space of a pair $kl$ using the PNO overlap matrices $S^{ij,kl}_{\bar{a}_{ij}\bar{b}_{kl}}$ or the respective matrices between ground and excited state PNOs.

As indicated in Table I, all steps which in a canonical implementation have operation counts scaling with $\mathcal{O}(\mathcal{N}^6)$ (the contributions $\rho^A_{\mu_2}$, $\rho^C_{\mu_2}$, and $\rho^D_{\mu_2}$) have in the PNO-based implementation a linear cost scaling. We currently still accept a cubic cost-scaling for the transformation of $E_{bc}$ and $\bar{E}_{bc}$ from the full virtual basis to the PNO basis since this step has a very small prefactor and does not yet contribute significantly

to the overall wall time. The computation of the $\bar{E}$ intermediates themselves (see Table III) in each iteration also scales as $\mathcal{O}(\mathcal{N}^3)$ but again with a small prefactor. For large-scale calculations, the $\mathcal{O}(\mathcal{N}^3)$-scaling transformations of the Coulomb and exchange integrals $(ik|l\bar{c}_{kj}) = \sum_\mu d^{kj}_{\mu\bar{c}_{kj}}(ik|l\mu)$ and $(il|k\bar{c}_{kj}) = \sum_\mu d^{kj}_{\mu\bar{c}_{kj}}(il|k\mu)$ from the AO the PNO basis dominate in the current implementation the overall costs during the iterations.

The calculation of the state-specific two-electron integrals $(\bar{a}\bar{c}|\bar{b}\bar{d})$ currently scales quadratically with the system size due to the calculation of $(Q|\mu\nu)$ in the full auxiliary basis $\{Q\}$. But also this step has a very small prefactor. The calculation of the 3-index PNO integrals $(Q|\bar{a}\bar{c})$, their density fitting, and the final contractions to $(\bar{a}\bar{c}|\bar{b}\bar{d})$ are done in a pair-specific auxiliary basis. These steps are linear scaling but have a large prefactor and currently dominate together with the computation of $W^{ij}_{Q\bar{d}^0\bar{a}}$ for small to medium sized systems the costs for the calculation of the state-specific intermediates after each PNO reconstruction. For larger systems, the computation of $(Q_{ij}|k\bar{d}^0_{ij}) = \sum_\mu (Q_{ij}|\mu\bar{d}^0_{ij})C_{\mu k}$ becomes dominant due to its $\mathcal{O}(\mathcal{N}^3)$ scaling. This is then the computationally most demanding contribution to the B terms $\rho^B_{\mu_2}$. But it should be mentioned that these integrals only need to be computed once as global intermediates since they do not depend on any excited state quantities in contrast to the $\mathcal{O}(\mathcal{N}^2)$ scaling intermediate $W^{ij}_{Q\bar{d}^0\bar{a}}$. The time-determining steps for large-scale applications are in our current implementation the generation of some $t_1$- and $R_1$-dressed integrals for the ring terms, $\rho^C_{\mu_2}$, $\rho^D_{\mu_2}$, and $\rho^B_{\mu_2}$. The computation of all other global, local, and state-specific intermediates for the Jacobian transformations scales at most quadratically with the system size.

### D. Solution of the eigenvalue problem in a PNO basis

For the solution of the eigenvalue problem, we use a single-state solver which determines the eigenvalues and eigenvectors of only one state at a time.[37] Because the space spanned by the excited state doubles amplitudes and thus the respective PNOs depend on the excited state singles amplitudes which are not known prior to solving the eigenvalue problem, we determine the PNOs in a self-consistent manner while solving the eigenvalue problem. Whenever the overlap $s = R^{(0)}_{\mu_1} R_{\mu_1}/(||R_{\mu_1}|| \cdot ||R^{(0)}_{\mu_1}||)$ between the singles part of the start vector $R^{(0)}_{\mu_1}$ for which the PNOs were constructed and the current singles guess $R_{\mu_1}$ significantly deviates from 1 so that

$$1 - s \geq 10 \cdot ||\sigma|| \tag{26}$$

is no longer fulfilled (where $\sigma$ denotes the residual vector of the eigenvalue problem), updated PNOs are generated and the Davidson procedure is restarted.

To obtain a suitable start guess for the doubles part of the eigenvector in the new PNO basis, the solution vector from the previous iteration is projected onto the new PNO basis. To enhance the convergence rate and minimize the number of PNO reconstructions for PNO-CCSD, a PNO-ADC(2) calculation followed by the perturbative correction PNO-ADC(2)-(D)[38] is carried out prior to the PNO-CCSD calculation. The PNO-ADC(2) eigenvectors are then resorted according to the PNO-ADC(2)-(D)[38] excitation energies and used as start for the PNO-CCSD excitation energy calculation.

## III. COMPUTATIONAL DETAILS

The calculation of PNO-CCSD excitation energies has been implemented in a development version of the pnoccsd program[31,34] of the TURBOMOLE package.[58] Hartree-Fock calculations have been carried out with the dscf program,[59] density functional theory (DFT)[60,61] geometry optimizations with ridft,[62–66] and canonical CCSD reference calculations with the ccsdf12 program of TURBOMOLE. For the DFT geometry optimizations of the alkene chains (see Sec. IV C), we have used the B3LYP functional,[67–71] the def2-TZVP orbital basis set,[72] and the corresponding auxiliary basis for the RI approximation of Coulomb integrals[73] (RI-J approximation). Test calculations have been done using the def2-TZVP,[72] cc-pVDZ,[74] and d-aug-cc-pVDZ[75] orbital basis sets. If not explicitly mentioned, the corresponding standard auxiliary basis sets[76,77] for the RI approximation of two electron integrals have been used in post-HF calculations. The occupied orbital basis has either been localized using Pipek-Mezey[78] localization or intrinsic bond orbitals (IBOs)[79] (*vide infra*). Furthermore, we used the frozen core approximation with the 1*s* orbitals of second row atoms excluded from the correlation treatment.

The thresholds for the pair correlation energy, $T_{pair}$, and the truncation of the OSV basis, $T_{\mathrm{OSV}}$, are coupled to the PNO truncation threshold, $T_{\mathrm{PNO}}$, as $T_{pair} = (0.1 \cdot T_{\mathrm{PNO}})^{2/3}$ and $T_{\mathrm{OSV}} = 0.1 \cdot T_{\mathrm{PNO}}$. In all calculations we use identical truncation thresholds for the ground and the excited states.

## IV. RESULTS

### A. Accuracy of PNO-CCSD

To investigate the accuracy of PNO-CCSD with respect to canonical CCSD we use the test set developed by Schreiber *et al.* in Ref. 80. It comprises 153 vertical singlet excitations in 28 organic molecules. The structures were taken from the supplementary material of Ref. 80.

The errors introduced by the PNO approximation were evaluated with respect to canonical CCSD as it is implemented in the ccsdf12 program in TURBOMOLE, where 4-index electron repulsion integrals are used for the ladder terms ($\rho^A_{\mu_2}$, $\rho^B_{\mu_2}$) and $\rho^F_{\mu_2}$ and the intermediates $E_{ki}$ and $\bar{E}_{ki}$ and the RI approximation is used for all remaining electron repulsion integrals. Test calculations showed that the deviations due to the different use of the RI approximation in the PNO-based and the canonical implementation are in the order of $10^{-3}$ – $10^{-4}$ eV and thus irrelevant for practical purposes.

TABLE II. Statistical measures for the errors in PNO-CCSD excitation energies in the def2-TZVP basis. The abbreviations ME, MAE, and MAX stand for mean error, mean absolute error, and maximum error, respectively, and $\sigma$ denotes the standard deviation with respect to the ME.

| | ME | MAE | MAX | $\sigma$ |
|---|---|---|---|---|
| $T_{\text{PNO}} = 10^{-6}$ | 0.040 | 0.041 | 0.089 | 0.022 |
| $T_{\text{PNO}} = 10^{-7}$ | 0.007 | 0.008 | 0.033 | 0.008 |
| $T_{\text{PNO}} = 10^{-8}$ | −0.002 | 0.003 | 0.011 | 0.003 |

Table II and Fig. 1 summarize the results obtained from a statistical analysis of the PNO truncation error for the CCSD excitation energies. All statistical measures decrease monotonically with the PNO threshold. The mean errors (ME) reveal that loose and moderate PNO thresholds ($T_{\text{PNO}} = 10^{-6}, 10^{-7}$) tend to slightly overestimate the excitation energies. Already with the moderate PNO threshold $T_{\text{PNO}} = 10^{-7}$ the mean absolute error (MAE) drops below 0.01 eV which is a promising result for a future implementation of PNO excitation energies for methods including connected triple excitations where such an accuracy is required to maintain the intrinsic accuracy of these methods.

Figure 2 compares mean absolute and maximum PNO truncation errors of PNO-CCSD to those for PNO-CC2 and PNO-ADC(2)-x. The latter were taken from Refs. 37 and 38. The comparison shows that both statistical measures are for PNO-ADC(2)-x much larger than for PNO-CC2 and PNO-CCSD; only for the loose threshold $T_{\text{PNO}} = 10^{-6}$ the MAE for PNO-CCSD and PNO-ADC(2)-x are close. In general, we observe that the PNO truncation errors for PNO-CCSD are only by a factor of two larger than for PNO-CC2 and that the convergence to the canonical results is for both methods almost identical. The fact that the errors for PNO-ADC(2)-x are substantially larger than for PNO-ADC(2) or PNO-CC2 has already been observed previously.[38] In Ref. 38, it was argued that this is caused by an unbalanced treatment of correlation effects from the ground and excited state wavefunctions

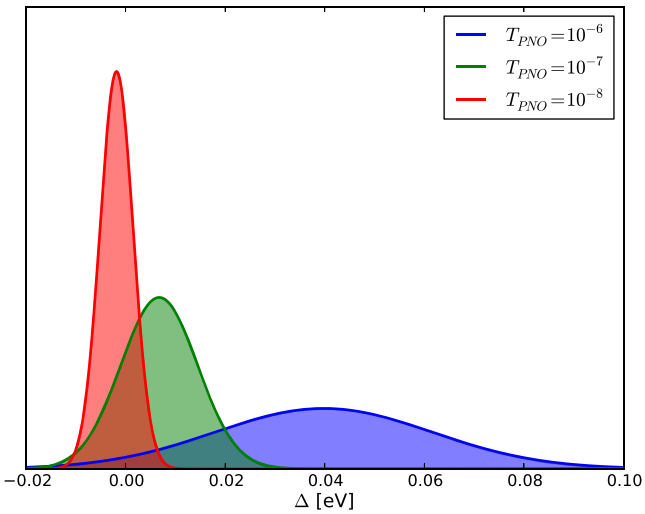



FIG. 1. Normal distributions of PNO errors in excitation energies from the test set of Schreiber *et al.*[80] (def2-TZVP basis).

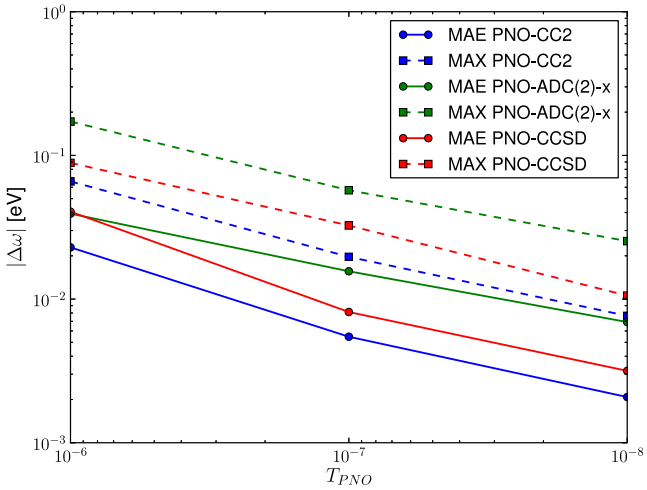



FIG. 2. Comparison of mean absolute and maximum errors of PNO-CC2, PNO-ADC(2)-x, and PNO-CCSD in the def2-TZVP basis.

on the excitation energies in the PNO-ADC(2)-x method. ADC(2)-x includes in the secular matrix $\langle\mu_2|[H,\tau_{\nu_2}]|\text{HF}\rangle$, which accounts for correlation effects from the excited state wavefunction on the excitation energy, but neglects its counterpart $\langle\mu_2|[[H,T_2],\tau_{\nu_1}]|\text{HF}\rangle$, which accounts for similar correlation effects from the ground state wavefunction on the excitation energy. Including only one of the two terms destroys an error balance between them which is reestablished at the PNO-CCSD level when both terms are included. As shown in Ref. 38, the unbalanced treatment of ground and excited state correlation effects in ADC(2)-x is also the source for the sizeable systematic red shift of ADC(2)-x excitation energies.

### B. Charge transfer and Rydberg excitations

Charge transfer (CT) excitations are a challenge for local correlation methods since these excitations are not only by definition non-local but pose for PNO-based methods in addition the problem that due to a very low rank of $R_{\mu_1}$ the PNO basis obtained from the non-negligible eigenpairs of the density in Eq. (21) is very small and thus inflexible.[37] For long range CT states, $R_{\mu_1}$ has usually only a rank of 1 so that

$$R^i_a \approx \beta_{a\sigma^v}\beta_{i\sigma^o}, \tag{27}$$

where $\beta_{i\sigma^o}$ are the coefficients of the occupied natural transition orbital (NTO) and $\beta_{a\sigma^v}$ are the coefficients of the virtual NTO. The $R_1$-dressed integrals $(ai|\bar{b}j)$ from which the doubles amplitudes and the densities for the PNO construction are evaluated become in this case

$$(ai|\bar{b}j) \approx P^{ij}_{ab}\left[\beta_{i\sigma^o}(a\sigma^v|bj) - \beta_{a\sigma^v}(\sigma^o i|bj)\right]. \tag{28}$$

They are non-negligible for only two kinds of pairs $ij$: Those where $i$ is close to the occupied NTO and $j$ is close to the virtual NTO or vice versa and those pairs where both $i$ and $j$ are close to the occupied NTO. The contribution $P^{ij}_{ab}\beta_{i\sigma^o}(a\sigma^v|bj)$ has a rank which can be as large as the number of virtuals (rank-V) in the electron acceptor chromophore but only contributes if one LMO is close to the virtual NTO and the other LMO is close to the occupied NTO. The contribution

$P^{ij}_{ab}\beta_{a\sigma^v}(\sigma^o i|bj)$ is of rank 1 and only non-negligible if both LMOs are close to the occupied NTO. If occupied and virtual NTOs are localized in the same chromophore, both terms contribute for all pairs close to this chromophore. For CT states where the virtual and the occupied NTO are spatially separated, in contrast, only rank-1 terms contribute to $(ai|bj)$ if both LMOs are close to the occupied NTO. For such rank-1 pairs, $(ai|bj)$ has only two non-negligible singular vectors and, hence, decreasing the PNO threshold will not enlarge the PNO basis for these pairs. To prevent that this effect limits the accuracy of PNO-based response calculations it is for the second-order methods CIS(D), ADC(2), and CC2 sufficient to ensure that the amplitudes, from which the density in Eq. (21) is computed, can converge to the correct limit which can be implemented, e.g., using a numerical Laplace transformation of the orbital energy denominators to avoid the neglect of off-diagonal elements of the Fock matrix.[37] For higher-order methods with a more complex doubles-doubles block of the secular matrix, it is, however, no longer feasible to ensure this convergence.

To investigate this problem at the PNO-CCSD level we chose the two lowest $\pi\pi^*$ CT states in the $C_2H_4\cdots C_2F_4$ model system in the cc-pVDZ basis and compared the convergence of the excitation energies with the PNO threshold with that for the two lowest lying local $\pi\pi^*$ excitations (LE). For these calculations, we used the large aug-cc-pVQZ auxiliary basis[76] to exclude that the analysis of the errors is affected by deviations from the different use of the RI approximation in the PNO and the canonical code. The black colored graphs in Fig. 3 show the results obtained for PNO-CCSD using the Laplace transformation (as implemented for PNO-CC2) for rank-1 pairs. Apparently, the LE states show errors and a convergence behavior very similar to the one observed for the Schreiber test set. For the $\pi_{C_2H_4} \rightarrow \pi^*_{C_2F_4}$ CT transition, the PNO truncation error decays similarly fast as for the LE states. For the $\pi_{C_2F_4} \rightarrow \pi^*_{C_2H_4}$ CT transition, the PNO truncation errors are significantly larger than for the other states and the convergence is much slower. That the results for the $\pi_{C_2F_4} \rightarrow \pi^*_{C_2H_4}$ transition are more sensitive to the PNO construction for the rank-1 pairs than the results for the other CT transition is due to the fact that for this transition the occupied NTO is located at $C_2F_4$ which has far more LMOs than $C_2H_4$ and, hence, the number of rank-1 pairs is much larger than for the $\pi_{C_2H_4} \rightarrow \pi^*_{C_2F_4}$ transition.

The red colored graphs in Fig. 3 show the results obtained using for rank-1 pairs the pre-PNO basis without further truncation of the virtual space, i.e., using for these pairs the pre-PNO basis as PNO basis.

That the error for the $\pi_{C_2H_4} \rightarrow \pi^*_{C_2F_4}$ transition is exceptionally small for $T_{PNO} = 10^{-7}$ but for $T_{PNO} = 10^{-8}$ again of the same order of magnitude as for the $\pi_{C_2H_4} \rightarrow \pi^*_{C_2F_4}$ transition is due to a fortunate error cancellation for this particular state and threshold. Figure 3 shows that the accuracy of the LE states is not affected by using the pre-PNOs without further truncation (due to the absence of rank-1 pairs). For both CT states, the errors are significantly reduced and decay rapidly.

We also investigated the accuracy of the excited state PNO construction for Rydberg states, which is a second class of non-local transitions where the occupied and virtual NTOs are located in different regions of space. As show case we chose the lowest lying Rydberg state ($1^1A$) of 1,1,2-trifluoro-1-hexene in the d-aug-cc-pVDZ[75] basis. For the occupied orbitals, we used IBOs. The red colored graph in Fig. 4 shows the errors obtained when using for rank-1 pairs the pre-PNO basis without further truncation as described above and the black colored graph shows the MAE obtained for Schreiber's test set (compare Sec. IV A and Table II). The convergence behavior for the Rydberg state is essentially the same as for CT states: If for rank-1 pairs the pre-PNO basis is used without further truncations, the PNO truncation errors decrease fast with $T_{PNO}$.

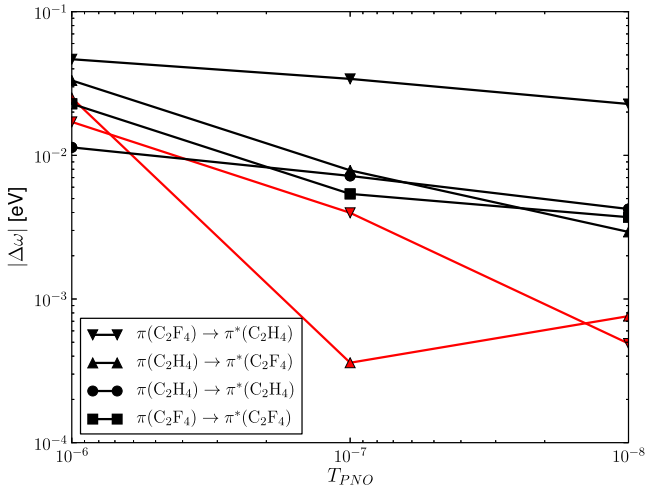



FIG. 3. Absolute errors in CT and LE states of $C_2H_4\cdots C_2F_4$ in the cc-pVDZ basis. The black lines show the results obtained with the PNO construction proposed in Ref. 37 for second-order methods. The red lines show the absolute error obtained by keeping for rank-1 pairs the pre-PNO basis without further truncation. For the LE states, there are no red lines visible since these are congruent with the black lines (due to the absence of rank-1 pairs).

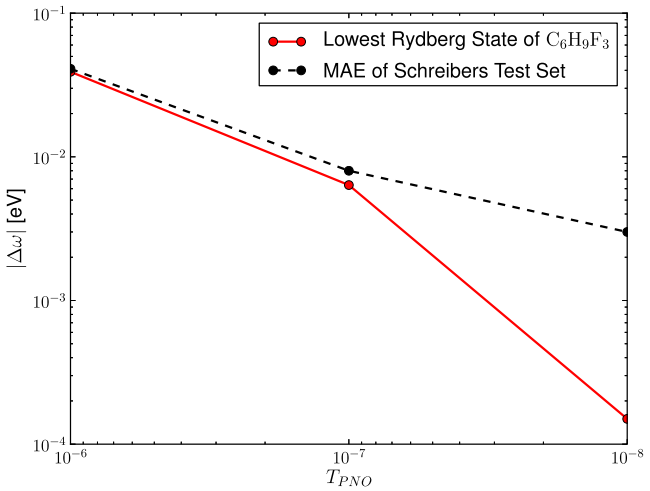



FIG. 4. Absolute errors of the first Rydberg state ($1^1A$) of 1,1,2-trifluoro-1-hexene in the d-aug-cc-pVDZ basis compared to the MAE obtained for Schreiber's test set (see Sec. IV A).

The results suggest that for rank-1 pairs the pre-PNO basis presents a simple and efficient possibility to obtain a PNO space which is flexible enough to allow for a reliable and rapid convergence of the PNO truncation errors in excitation energy calculations with higher-order methods. The identification of the rank-1 pairs is a simple and cheap black-box procedure described in Ref. 37. It should at this point be stressed that already the number of pre-PNOs scales linearly with the chromophore size. Hence, using for rank-1 pairs the pre-PNO basis without further truncation does not affect the scaling of the computational costs and increases the prefactor only insignificantly.

### C. Performance of the implementation

To investigate the performance of the PNO-CCSD implementation for excitation energies we carried out calculations on alkene chains in the def2-TZVP basis set using IBOs for the occupied space. Figure 5 shows the wall times obtained for thread-parallel calculations on a machine with 2 Intel Xeon E5-2609 8-Core CPUs for the well-parallelized canonical CCSD code and the yet only partially parallelized PNO-CCSD implementation.

The Jacobian transformations for canonical CCSD scale for the largest systems as $\mathcal{O}\left(\mathcal{N}^{5.59}\right)$ with the chain size. In the PNO-CCSD implementation, the scaling is reduced to $\mathcal{O}\left(\mathcal{N}^{2.87}\right)$ (obtained from the last two points shown in Fig. 5). The time-determining steps in both the canonical and the PNO-CCSD calculations arise from the same terms but for different reasons: For canonical CCSD calculations on small- to medium-sized molecules, the calculation of the B term $\rho^B_{\mu_2}$ represents the time-determining step, while for larger systems this term becomes negligible compared to the ring terms C and D ($\rho^C_{\mu_2}$, $\rho^D_{\mu_2}$) due to an asymptotic $\mathcal{O}\left(\mathcal{N}^4\right)$-scaling for

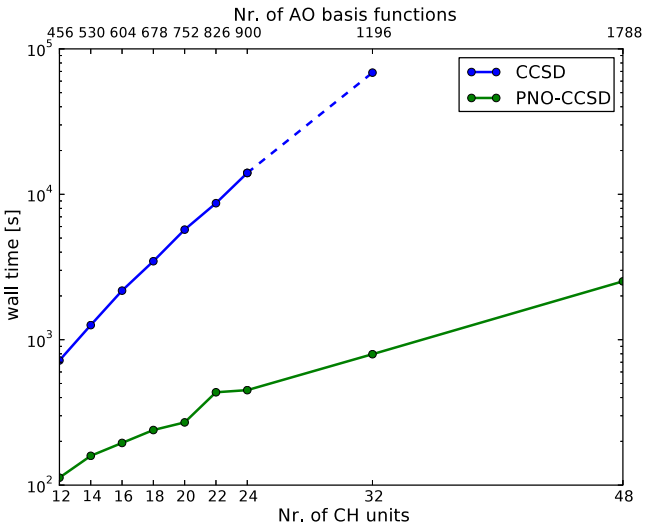



FIG. 5. Wall-time of a single Jacobian transformation for canonical and PNO-CCSD for alkene chains $C_nH_{n+2}$ in the def2-TZVP basis. The calculations have been done Open-MP parallel on 2 Intel Xeon E5-2609 8-Core CPUs (1.7 GHz) and 64 GB of Ram. For the PNO-CCSD calculations, a PNO threshold of $10^{-7}$ has been used. The dashed line for canonical CCSD was obtained by an extrapolation according to the power law $4.4 \cdot 10^{-13} \cdot \mathcal{N}_{bf}^{5.59}$, where $\mathcal{N}_{bf}$ denotes the number of basis functions (for details see text).

the contraction $\sum_{\mu\nu} t^{ij}_{\mu\nu}(\mu\kappa|\nu\lambda)$ which is evaluated in the AO basis. For large calculations, the strictly $\mathcal{O}\left(\mathcal{N}^6\right)$-scaling C and D terms become time-determining. For PNO-CCSD, the evaluation of the B terms also has a large prefactor and is time-determining for medium-sized molecules but these contributions soon become linear and quadratic scaling since they are rather short-ranged.[81] For larger systems, the time-determining step in our current PNO-CCSD implementation is the evaluation of the $R_1$-dressed integral matrices $\mathbf{J}^{R1o}$ and $\mathbf{L}^{R1o}$ in the PNO basis (compare Table III in the Appendix) which has a cubic cost-scaling. For example, for $C_{48}H_{50}$, about 50% of the wall time is spent for the calculation of these integrals. But still, the PNO-CCSD implementation performs impressingly well even when taking the computational costs for the PNO reconstruction and the recalculation of the state-specific intermediates into account. For example, for $C_{32}H_{34}$, the PNO-CCSD excitation energy calculation was completed before a single canonical CCSD ground state iteration was finished.

## V. SUMMARY AND CONCLUSIONS

We presented an efficient and accurate implementation of PNO-CCSD for the calculation of vertical excitation energies. Using state-specific PNOs to solve the excited state eigenvalue problem it could be demonstrated that the wall time for the Jacobian transformations scales at most cubically with the chromophore size and that PNO-CCSD outperforms canonical CCSD even for small molecular systems. For long-range charge transfer states, a smooth convergence with $T_{\mathrm{PNO}}$ is ensured by using for the problematic rank-1 pairs the pre-PNO basis, which is obtained from merging the OSVs of the respective LMOs without further truncation. This does not affect the scaling of the computational costs with the system size since already the pre-PNO basis scales linearly with the chromophore size.

We find a fast decay of the PNO truncation errors with the cutoff threshold. Already with a moderate threshold of $T_{\mathrm{PNO}} = 10^{-7}$ the mean absolute error in the excitation energies for a test set of 153 singlet excitations in 28 organic molecules decayed blow 0.01 eV. These are much smaller errors than observed previously for PNO-ADC(2)-x, for which apparently the unbalanced treatment of correlation effects from the ground and the excited state wavefunction retards the convergence with the PNO cutoff threshold.

These findings are encouraging for a future development of PNO-based iterative and perturbative triples methods such as CC3[82,83] and CCSDR(T) or CCSDR(3)[84] for highly accurate excitation energies which require PNO truncation errors of less than 0.01 eV to exploit the full accuracy of these methods.

## ACKNOWLEDGMENTS

This work has been supported by the Deutsche Forschungsgemeinschaft (DFG) under Grant No. HA 2588/7.

## APPENDIX: DEFINITION OF INTERMEDIATES FOR THE PNO-CCSD JACOBIAN RIGHT TRANSFORMATION

TABLE III. Global and local intermediates needed for the CCSD Jacobian right transformation. For ease of notation, the short-hand notation $L^{pq}_{rs} = 2(pr|qs) - (pq|rs)$ is used.

| Global | Local |
|---|---|
| $E_{ki} = \hat{F}_{ki} + \sum_{j\bar{a}^0\bar{b}^0} \tilde{t}^{ij}_{\bar{a}^0\bar{b}^0} \sum_{\bar{c}^0\bar{d}^0} S^{ij,jk}_{\bar{b}^0\bar{c}^0} (\bar{c}^0 j|\bar{d}^0 k) S^{jk,ij}_{\bar{d}^0\bar{a}^0}$ | $\bar{E}_{ki} = \bar{F}_{ki} + \sum_{j\bar{a}\bar{b}} \bar{R}^{ij}_{\bar{a}\bar{b}} \sum_{\bar{c}^0\bar{d}^0} S^{ij,jk}_{\bar{b}\bar{c}^0} (\bar{c}^0 j|\bar{d}^0 k) S^{jk,ij}_{\bar{d}^0\bar{a}}$ |
| | $\bar{F}_{ki} = \sum_c \hat{F}_{kc} R^i_c + \sum_{\mu\nu} \Lambda^p_{\mu k} \Lambda^h_{\nu i} \tilde{F}_{\mu\nu}$ |
| $E_{bc} = \hat{F}_{bc} - \sum_{ij\bar{b}^0} d^{ij}_{b\bar{b}^0} \sum_{\bar{d}^0} \tilde{t}^{ij}_{\bar{b}^0\bar{d}^0} \sum_{\bar{c}^0} K^{kj}_{\bar{d}^0\bar{c}^0} d^{ij}_{c\bar{c}^0}$ | $\bar{E}_{bc} = \bar{F}_{bc} - \sum_{ij\bar{b}} d^{ij}_{b\bar{b}} \sum_{\bar{c}^0} d^{kj}_{c\bar{c}^0} \sum_{\bar{d}} \tilde{R}^{ij}_{\bar{b}\bar{d}} \sum_{\bar{d}^0} K^{kj}_{\bar{d}^0\bar{c}^0} S^{kj,ij}_{\bar{d}^0\bar{d}}$ |
| | $\bar{F}_{bc} = -\sum_j R_{bj} \hat{F}_{jc} + \sum_{\mu\nu} \tilde{F}_{\mu\nu} \Lambda^p_{\mu b} \Lambda^h_{\nu c}$ |
| | $\tilde{F}_{\mu\nu} = \sum_{dl} [2(\mu\nu|ld) - (\mu d|l\nu)] R_{dl}$ |
| $\Gamma^{T_2,+E,ij}_{kl} = (ik\hat{\|}jl) - \delta_{ki} E_{lj} - \delta_{lj} E_{ki} + \sum_{\bar{c}^0\bar{d}^0} t^{ij}_{\bar{c}^0\bar{d}^0} \sum_{\bar{c}'^0\bar{d}'^0} S^{ij,kl}_{\bar{c}^0\bar{c}'^0} (\bar{c}'^0 k|\bar{d}'^0 l) S^{kl,ij}_{\bar{d}'^0\bar{d}^0}$ | $\Gamma^{R_2,+\bar{E},ij}_{kl} = (ik\bar{\|}jl) - \delta_{ki} \bar{E}_{lj} - \delta_{lj} \bar{E}_{ki} + \sum_{\bar{c}\bar{d}} R^{ij}_{\bar{c}\bar{d}} \sum_{\bar{c}'^0\bar{d}'^0} S^{ij,kl}_{\bar{c}\bar{c}'^0} (\bar{c}'^0 k|\bar{d}'^0 l) S^{kl,ij}_{\bar{d}'^0\bar{d}}$ |
| | $\bar{C}_{\bar{a}_{ij}\bar{c}^0_{kj}} = J^{R1o,ik}_{\bar{a}_{ij}\bar{c}^0_{kj}} + \sum_{\bar{a}'\bar{c}'} S^{ij,ki}_{\bar{a}_{ij}\bar{a}'_{ik}} C^{R2,ik}_{\bar{a}'_{ik}\bar{c}'_{ik}} S^{ki,kj}_{\bar{c}'_{ik}\bar{c}^0_{kj}}$ |
| | $\bar{D}_{\bar{a}_{ij}\bar{c}^0_{kj}} = L^{R1o,ik}_{\bar{a}_{ij}\bar{c}^0_{kj}} + \sum_{\bar{a}'\bar{c}'} S^{ij,ki}_{\bar{a}_{ij}\bar{a}'_{ik}} D^{R2,ik}_{\bar{a}'_{ik}\bar{c}'_{ik}} S^{ki,kj}_{\bar{c}'_{ik}\bar{c}^0_{kj}}$ |
| $C^{T2,ik}_{\bar{a}^0_{ik}\bar{c}^0_{ik}} = -\frac{1}{2} \sum_{l\bar{a}^0_{li}\bar{d}^0_{li}} (\bar{c}^0_{ki} l|\bar{d}^0_{li} k) \left( t^{li}_{\bar{a}^0_{li}\bar{d}^0_{li}} + 2 t^l_{\bar{a}^0_{li}} t^i_{\bar{d}^0_{li}} \right) S^{li,ik}_{\bar{a}^0_{li}\bar{a}^0_{ik}} + J^{T1v,ik}_{\bar{a}^0_{ik}\bar{c}^0_{ik}}$ | $C^{R2,ik}_{\bar{a}_{ik}\bar{c}_{ik}} = -\frac{1}{2} \sum_{l\bar{a}_{li}\bar{d}_{li}} (\bar{c}_{ki} l|\bar{d}_{li} k) \left( R^{li}_{\bar{a}_{li}\bar{d}_{li}} + 2 R^l_{\bar{a}_{li}} t^i_{\bar{d}_{li}} + 2 t^l_{\bar{a}_{li}} R^i_{\bar{d}_{li}} \right) S^{li,ik}_{\bar{a}^0_{li}\bar{a}_{ik}} + J^{R1v,ik}_{\bar{a}_{ik}\bar{c}_{ik}}$ |
| $D^{T2,ik}_{\bar{a}^0_{ik}\bar{c}^0_{ik}} = \frac{1}{2} \sum_{l\bar{a}^0_{li}\bar{d}^0_{li}} L^{k\bar{d}^0_{li}}_{\bar{c}^0_{ki} l} \left( t^{li}_{\bar{a}^0_{li}\bar{d}^0_{li}} - 2 t^l_{\bar{a}^0_{li}} t^i_{\bar{d}^0_{li}} \right) S^{li,ik}_{\bar{a}^0_{li}\bar{a}^0_{ik}} + L^{T1v,ik}_{\bar{a}^0_{ik}\bar{c}^0_{ik}}$ | $D^{R2,ik}_{\bar{a}_{ik}\bar{c}_{ik}} = \frac{1}{2} \sum_{l\bar{a}_{li}\bar{d}_{li}} L^{k\bar{d}_{li}}_{\bar{c}_{ki} l} \left( R^{li}_{\bar{a}_{li}\bar{d}_{li}} - 2 R^l_{\bar{a}_{li}} t^i_{\bar{d}_{li}} - 2 t^l_{\bar{a}_{li}} R^i_{\bar{d}_{li}} \right) S^{li,ik}_{\bar{a}^0_{li}\bar{a}_{ik}} + L^{R1v,ik}_{\bar{a}_{ik}\bar{c}_{ik}}$ |
| | $J^{R1o,ik}_{\bar{a}_{ij}\bar{c}^0_{kj}} = -\sum_l R^l_{\bar{a}_{ij}} \sum_{\mu} d^{kj}_{\mu\bar{c}^0_{kj}} (ik|l\mu)$ |
| | $L^{R1o,ik}_{\bar{a}_{ij}\bar{c}^0_{kj}} = -2 \sum_l R^l_{\bar{a}_{ij}} \sum_{\mu} d^{kj}_{\mu\bar{c}^0_{kj}} (il|k\mu) - J^{R1o,ik}_{\bar{a}_{ij}\bar{c}^0_{kj}}$ |
| $J^{T1v,ik}_{\bar{a}^0_{ik}\bar{c}^0_{ik}} = \sum_{\bar{d}^0_{ik}} (i\bar{d}^0_{ik}|\bar{a}^0_{ik}\bar{c}^0_{ik}) \sum_d d^{ik}_{d\bar{d}^0_{ik}} t^k_d$ | $J^{R1v,ik}_{\bar{a}_{ik}\bar{c}_{ik}} = \sum_{\bar{d}_{ik}} (i\bar{d}_{ik}|\bar{a}_{ik}\bar{c}_{ik}) \sum_d d^{ik}_{d\bar{d}_{ik}} R^k_d$ |
| $L^{T1v,ik}_{\bar{a}^0_{ik}\bar{c}^0_{ik}} = 2 \sum_{\bar{d}^0_{ik}} (i\bar{a}^0_{ik}|\bar{d}^0_{ik}\bar{c}^0_{ik}) \sum_d d^{ik}_{d\bar{d}^0_{ik}} t^k_d - J^{T1v,ik}_{\bar{a}^0_{ik}\bar{c}^0_{ik}}$ | $L^{R1v,ik}_{\bar{a}_{ik}\bar{c}_{ik}} = 2 \sum_{\bar{d}_{ik}} (i\bar{a}_{ik}|\bar{d}_{ik}\bar{c}_{ik}) \sum_d d^{ik}_{d\bar{d}_{ik}} R^k_d - J^{R1v,ik}_{\bar{a}_{ik}\bar{c}_{ik}}$ |
| | $\Omega^{B(R2),ij}_{\bar{a}k} = \sum_{\bar{c}\bar{d}} (\bar{a}\bar{c}|k\bar{d}) R^{ij}_{\bar{c}\bar{d}}$ |

TABLE IV. State-specific intermediates needed for the CCSD Jacobian right transformation. For ease of notation, the short-hand notation $L^{pq}_{rs} = 2(pq|rs) - (ps|rq)$ is used.

| |
|---|
| $C_{\bar{a}_{ij}\bar{c}_{kj}} = J^{T1o,ki}_{\bar{a}_{ij}\bar{c}_{kj}} + \sum_{\bar{a}^0\bar{c}^0} S^{ij,ki}_{\bar{a}_{ij}\bar{a}^0_{ki}} C^{T2,ik}_{\bar{a}^0\bar{c}^0} S^{ki,kj}_{\bar{c}^0_{ki}\bar{c}_{kj}}$ |
| $D_{\bar{a}_{ij}\bar{c}_{kj}} = L^{T1o,ki}_{\bar{a}_{ij}\bar{c}_{kj}} + \sum_{\bar{a}^0\bar{c}^0} S^{ij,ki}_{\bar{a}_{ij}\bar{a}^0_{ki}} D^{T2,ik}_{\bar{a}^0\bar{c}^0} S^{ki,kj}_{\bar{c}^0_{ki}\bar{c}_{kj}}$ |
| $J^{T1o,ik}_{\bar{a}_{ij}\bar{c}_{kj}} = (ik|\bar{a}_{ij}\bar{c}_{kj}) - \sum_l t^l_{\bar{a}_{ij}} \sum_{\mu} d^{kj}_{\mu\bar{c}_{kj}} (ik|l\mu)$ |
| $L^{T1o,ik}_{\bar{a}_{ij}\bar{c}_{kj}} = L^{ik}_{\bar{a}_{ij}\bar{c}_{kj}} - 2 \sum_l t^l_{\bar{a}_{ij}} \sum_{\mu} d^{kj}_{\mu\bar{c}_{kj}} (il|k\mu) + \sum_l t^l_{\bar{a}_{ij}} \sum_{\mu} d^{kj}_{\mu\bar{c}_{kj}} (ik|l\mu)$ |
| $\Omega^{B(T2),ij}_{k\bar{a}} = \sum_{P_{ij}Q_{ij}} \sum_{\bar{d}^0} W^{ij}_{P_{ij}\bar{d}^0\bar{a}} \left[\mathbf{V}^{-1}\right]_{P_{ij}Q_{ij}} (Q_{ij}|k\bar{d}^0)$ |
| $W^{ij}_{Q_{ij}\bar{d}^0\bar{a}} = \sum_{\mu\nu} (Q_{ij}|\mu\nu) t^{ij}_{\mu\bar{d}^0} \Lambda^{p,ij}_{\nu\bar{a}}$ |

[1]P. Pulay, Chem. Phys. Lett. **100**, 151 (1983).
[2]S. Saebø and P. Pulay, Chem. Phys. Lett. **113**, 13 (1985).
[3]S. Saebø and P. Pulay, Annu. Rev. Phys. Chem. **44**, 213 (1993).
[4]P. Pulay and S. Saebø, Theor. Chim. Acta **69**, 357 (1986).
[5]S. Saebø and P. Pulay, J. Chem. Phys. **86**, 914 (1987).
[6]S. Saebø and P. Pulay, J. Chem. Phys. **88**, 1884 (1988).
[7]G. Rauhut, P. Pulay, and H.-J. Werner, J. Comput. Chem. **19**, 1241 (1998).
[8]M. Schütz, G. Hetzer, and H.-J. Werner, J. Chem. Phys. **111**, 5691 (1999).
[9]C. Hampel and H.-J. Werner, J. Chem. Phys. **104**, 6286 (1996).
[10]M. Schütz, Phys. Chem. Chem. Phys. **4**, 3941 (2002).
[11]M. Schütz and F. R. Manby, Phys. Chem. Chem. Phys. **5**, 3349 (2003).
[12]M. Schütz and H.-J. Werner, Chem. Phys. Lett. **318**, 370 (2000).
[13]H.-J. Werner, P. J. Knowles, G. Knizia, F. R. Manby, and M. Schütz, Wiley Interdiscip. Rev.: Comput. Mol. Sci. **2**, 242 (2012).
[14]W. Meyer, *Methods of Electronic Structure Theory*, 3rd ed. (Plenum Press, New York, 1977).
[15]W. Meyer, Theor. Chem. Acc. **35**, 277 (1974).
[16]W. Meyer, J. Chem. Phys. **58**, 1017 (1973).
[17]W. Meyer, Int. J. Quantum Chem. **S5**, 341 (1971).
[18]R. Ahlrichs, F. Driessler, H. Lischka, V. Staemmler, and W. Kutzelnigg, J. Chem. Phys. **62**, 1235 (1975).
[19]R. Ahlrichs and F. Driessler, Theor. Chem. Acc. **36**, 275 (1975).
[20]V. Staemmler and R. Jaquet, Theor. Chem. Acc. **59**, 487 (1981).
[21]J. L. Whitten, J. Chem. Phys. **58**, 4496 (1973).
[22]B. I. Dunlap, J. W. D. Conolly, and J. R. Sabin, J. Chem. Phys. **71**, 3396 (1979).
[23]F. Neese, A. Hansen, and D. G. Liakos, J. Chem. Phys. **131**, 064103 (2009).
[24]F. Neese, A. Hansen, F. Wennmohs, and S. Grimme, Acc. Chem. Res. **42**, 641 (2009).
[25]F. Neese, F. Wennmohs, and A. Hansen, J. Chem. Phys. **130**, 114108 (2009).
[26]D. G. Liakos, A. Hansen, and F. Neese, J. Chem. Theory Comput. **7**, 76 (2011).
[27]A. Hansen, D. G. Liakos, and F. Neese, J. Chem. Phys. **135**, 214102 (2011).
[28]C. Riplinger and F. Neese, J. Chem. Phys. **138**, 034106 (2013).
[29]C. Krause and H.-J. Werner, Phys. Chem. Chem. Phys. **14**, 7591 (2012).
[30]C. Hättig, D. P. Tew, and B. Helmich, J. Chem. Phys. **136**, 204105 (2012).
[31]G. Schmitz, B. Helmich, and C. Hättig, Mol. Phys. **111**, 2463 (2013).
[32]J. Yang, G. K. L. Chan, F. R. Manby, M. Schütz, and H.-J. Werner, J. Chem. Phys. **136**, 144105 (2012).
[33]D. P. Tew and C. Hättig, Int. J. Quantum Chem. **113**, 224 (2013).
[34]G. Schmitz, C. Hättig, and D. P. Tew, Phys. Chem. Chem. Phys. **16**, 22167 (2014).
[35]G. Schmitz and C. Hättig, J. Chem. Phys. **145**, 234107 (2016).
[36]B. Helmich and C. Hättig, J. Chem. Phys. **135**, 214106 (2011).
[37]B. Helmich and C. Hättig, J. Chem. Phys. **139**, 084114 (2013).
[38]B. Helmich and C. Hättig, Comput. Theor. Chem. **1040-1041**, 35 (2014).
[39]O. Christiansen, H. Koch, and P. Jørgensen, Chem. Phys. Lett. **243**, 409 (1995).
[40]D. Kats, T. Korona, and M. Schütz, J. Chem. Phys. **125**, 104106 (2006).
[41]T. Korona and H.-J. Werner, J. Chem. Phys. **118**, 3006 (2003).
[42]T. D. Crawford and R. A. King, Chem. Phys. Lett. **366**, 611 (2002).
[43]A. K. Dutta, F. Neese, and R. Izsák, J. Chem. Phys. **145**, 034102 (2016).
[44]R. H. Myhre, A. M. J. Sánchez de Merás, and H. Koch, J. Chem. Phys. **141**, 224105 (2014).
[45]R. H. Myhre and H. Koch, J. Chem. Phys. **145**, 044111 (2016).
[46]D. Mester, P. R. Nagy, and M. Kállay, J. Chem. Phys. **146**, 194102 (2017).
[47]P. Baudin and K. Kristensen, J. Chem. Phys. **144**, 224106 (2016).
[48]O. Christiansen, H. Koch, A. Halkier, P. Jørgensen, T. Helgaker, and A. Sánchez de Merás, J. Chem. Phys. **105**, 6921 (1996).
[49]G. D. Purvis and R. J. Bartlett, J. Chem. Phys. **76**, 1910 (1982).
[50]T. J. Lee and R. J. Rice, Chem. Phys. Lett. **150**, 406 (1988).
[51]G. E. Scuseria, C. L. Janssen, and H. L. Schaefer III, J. Chem. Phys. **89**, 7382 (1988).
[52]J. F. Stanton, J. Gauss, J. D. Watts, and R. J. Bartlett, J. Chem. Phys. **94**, 4334 (1991).
[53]C. Hampel, K. A. Peterson, and H.-J. Werner, Chem. Phys. Lett. **190**, 1 (1992).
[54]H. Koch, O. Christiansen, R. Kobayashi, P. Jørgensen, and T. Helgaker, Chem. Phys. Lett. **228**, 233 (1994).
[55]H. Koch and P. Jørgensen, J. Chem. Phys. **93**, 3333 (1990).
[56]E. R. Davidson, J. Comput. Phys. **17**, 87 (1975).
[57]B. Helmich, "Paarspezifische natürliche orbitale zur effizienten berechnung von coupled-cluster-anregungsenergien," Ph.D. thesis, Ruhr-Universität Bochum, 2014.
[58]R. Ahlrichs, M. Bär, M. Häser, H. Horn, and C. Kälmel, Chem. Phys. Lett. **162**, 165 (1989).
[59]M. Häser and R. Ahlrichs, J. Comput. Chem. **10**, 104 (1989).
[60]P. Hohenberg and W. Kohn, Phys. Rev. **136**, B864 (1964).
[61]W. Kohn and L. J. Sham, Phys. Rev. **140**, A1133 (1965).
[62]M. Von Arnim and R. Ahlrichs, J. Comput. Chem. **19**, 1746 (1998).
[63]M. Sierka, A. Hogekamp, and R. Ahlrichs, J. Chem. Phys. **118**, 9136 (2003).
[64]F. Weigend, J. Comput. Chem. **29**, 167 (2008).
[65]F. Weigend, Phys. Chem. Chem. Phys. **8**, 1057 (2006).
[66]F. Weigend, Phys. Chem. Chem. Phys. **4**, 4285 (2002).
[67]P. A. M. Dirac, Proc. R. Soc. London, Ser. A **123**, 714 (1929).
[68]J. C. Slater, Phys. Rev. **81**, 385 (1951).
[69]C. Lee, W. Yang, and G. Parr, Phys. Rev. B **37**, 785 (1988).
[70]A. D. Becke, Phys. Rev. A **38**, 3098 (1988).
[71]A. D. Becke, J. Chem. Phys. **98**, 5648 (1993).
[72]F. Weigend and R. Ahlrichs, Phys. Chem. Chem. Phys. **7**, 3297 (2005).
[73]K. Eichkorn, F. Weigend, O. Treutler, and R. Ahlrichs, Theor. Chem. Acc. **97**, 119 (1997).
[74]T. H. Dunning, J. Chem. Phys. **90**, 1007 (1989).
[75]D. E. Woon and T. H. Dunning, Jr., J. Chem. Phys. **100**, 2975 (1994).
[76]F. Weigend, A. Köhn, and C. Hättig, J. Chem. Phys. **116**, 3175 (2002).
[77]F. Weigend, M. Häser, H. Patzelt, and R. Ahlrichs, Chem. Phys. Lett. **294**, 143 (1998).
[78]J. Pipek and P. Mezey, J. Chem. Phys. **90**, 4916 (1988).
[79]G. Knizia, J. Chem. Theory Comput. **9**, 4834 (2013).
[80]M. Schreiber, M. R. Silva-Junior, S. P. A. Sauer, and W. Thiel, J. Chem. Phys. **128**, 134110 (2008).
[81]M. Schwilk, D. Usvyat, and H.-J. Werner, J. Chem. Phys. **142**, 121102 (2015).
[82]H. Koch, O. Christiansen, P. Jørgensen, A. M. J. Sánchez de Méras, and T. Helgaker, J. Chem. Phys. **106**, 1808 (1997).
[83]O. Christiansen, H. Koch, and P. Jørgensen, J. Chem. Phys. **103**, 7429 (1995).
[84]O. Christiansen, H. Koch, and P. Jørgensen, J. Chem. Phys. **105**, 1451 (1996).